Clin. Lab. 2022;68:XXX-XXX

ORIGINAL ARTICLE

MiR-641 Exacerbates the Progression of Ischemic Stroke Through the MCL-1/Wnt/β-Catenin Pathway

Qi Pan [#, 1, 2], Kaixuan Li [#, 3], Linxia Xue [4], Xiaoyi Cheng [2], Qi Zhou [4]

[#] *These authors contributed equally to this manuscript*
[1] *Shaanxi Key Laboratory of Brain Disorders, Xi'an Medical University, Xi'an, Shaanxi, China*
[2] *Department of Medical Imaging, The Second Affiliated Hospital of Xi'an Medical University, Xi'an, Shaanxi, China*
[3] *Department of Laboratory, The Second Affiliated Hospital of Xi'an Medical University, Xi'an, Shaanxi, China*
[4] *Department of Neurology, The Second Affiliated Hospital of Xi'an Medical University, Xi'an, Shaanxi, China*

SUMMARY

Background: **Ischemic stroke refers to ischemic necrosis or softening of limited brain tissue caused by ischemia and hypoxia due to impaired blood circulation in the brain. Ischemic stroke is a major classification of cerebrovascular disease, accounting for about 80% of patients with cerebrovascular disease in China, with a high rate of disability and death. Recently, miRNAs were reported to participate in ischemic stroke pathogenesis and development. In the study, we aimed to study the role and underlying mechanism of miR-641 in ischemic stroke.**
Methods: **Serum samples were extracted from acute ischemic stroke (AIS) patients and healthy controls. The oxygen-glucose deprivation/reoxygenation (OGD/R) method was used to treat SH-SY5Y cells to construct an ischemic stroke *in vitro* model. Real-time quantitative polymerase chain reaction (qRT-PCR) assay and western blot analysis were conducted to detect miR-641 and MCL-1 expressions. The targeted relationship between miR-641 and MCL-1 was confirmed by dual-luciferase reporter, RNA pull-down, and rescue assays. CCK-8, flow cytometry, and ELISA assays were performed to measure cell viability, apoptosis, and inflammation. The activation of the Wnt/β-catenin pathway was verified by western blot assay.**
Results: **MiR-641 was increased while MCL-1 was decreased in serum samples from AIS patients, serving as highly-sensitive biomarkers in AIS diagnosis. After OGD/R treatment, SH-SY5Y cell viability, and MCL-1 expression were decreased, along with increased miR-641 expression, cell apoptosis, and inflammation. MiR-641 aggravated while MCL-1 mitigated OGD/R-triggered injury and inflammation in SH-SY5Y cells. MCL-1 was a downstream target of miR-641, which could be negatively regulated by miR-641. Finally, miR-641 exacerbated the progression of OGD/R-triggered SH-SY5Y cell injury via the MCL-1/Wnt/β-catenin pathway.**
Conclusions: **MiR-641 may be a novel therapeutic agent for ischemic stroke by modulating the MCL-1/Wnt/β-catenin axis on neuronal damage in brain tissue in the ischemic region after ischemic stroke.**
(Clin. Lab. 2022;68:xx-xx. DOI: 10.7754/Clin.Lab.2021.210834)

Correspondence:
Qi Zhou
Department of Neurology
The Second Affiliated Hospital of Xi'an Medical University
No.167, Fangdong Street
Baqiao District, Xi'an 710038
Shaanxi
China
Email: zq15902926849@163.com

Manuscript accepted November 26, 2021

KEY WORDS

miR-641, MCL-1, Wnt/β-catenin, ischemic stroke

INTRODUCTION

Ischemic stroke is one of the major life-threatening diseases affecting human health in the world today [1]. To date, the most effective treatment for acute ischemic stroke (AIS) is revascularization therapy [2]. However, due to the narrow time window of revascularization

therapy and the secondary ischemia-reperfusion injury in the ischemic hemispheric zone, the results of revascularization therapy are not yet satisfactory [3]. Therefore, exploring biological markers for early diagnosis of ischemic stroke and studying their potential mechanisms can help to improve the limitations and side effects of revascularization therapy to some extent.

MicroRNAs (miRNAs) are a class of endogenous short-stranded non-coding RNAs that can influence the stability of mRNAs and regulate the transcription and translation of downstream mRNAs [4]. MiRNAs function by partial or complete complementary pairing with bases in the 3'UTR region of mRNAs of downstream target genes. Recently, studies have found that miR-641 is associated with the development of a variety of tumors, including lung cancer [5], gastric cancer [6], ovarian cancer [7], cervical cancer [8], prostate cancer [9], pancreatic carcinoma [10], osteosarcoma [11], bladder cancer [12], cholangiocarcinoma [13] and hepatocellular carcinoma [14]. In addition, miR-641 was down-regulated in glioblastoma cells [15]. Furthermore, a previous study by He et al. [16] found that miR-641 expression was significantly up-regulated in ischemic stroke patients compared with healthy volunteers. Nevertheless, the existing studies have not elucidated the correlation between miR-641 and ischemic stroke progression.

This study examined the aberrant expressions of miR-641 and MCL-1 in AIS serum samples and SH-SY5Y cells after OGD/R injury. We also explored the potential mechanisms of miR-641 and MCL-1 in OGD/R injury that may affect cell viability, apoptosis, and inflammatory response, aiming to provide a new theoretical basis for the mechanism of ischemic stroke injury.

MATERIALS AND METHODS

Subject recruitment

Fifty-one patients with AIS who attended the Second Affiliated Hospital of Xi'an Medical University from October 2019 to December 2020 and 50 regular physical examination patients attending the Second Affiliated Hospital of Xi'an Medical University during the same period were collected. The enrolled patients met the diagnostic criteria for AIS. The diagnosis was made by two neurologists with extensive clinical experience, based on the clinical manifestations at the onset of the disease, physical examination, and imaging findings such as CT or MRI of the head. The National Institutes of Health Stroke Scale (NIHSS) was used to assess neurological deficits in the enrolled patients. Patients were treated with rt-PA intravenous thrombolysis at a 0.9 mg/kg dose as recommended by the guideline, with complete medical records. Inclusion criteria: 1) symptoms and signs of focal neurological deficits of first acute onset; 2) head CT excluding cerebral hemorrhage or head magnetic resonance examination to confirm new ischemic responsible intracranial lesions; 3) no contraindications for intravenous thrombolytic therapy in the acute phase in accordance with the indications. Exclusion criteria: 1) progressive stroke after thrombolysis; 2) intracranial hemorrhage or hematoma-type hemorrhagic transformation; 3) combined with severe complications such as massive gastrointestinal bleeding. After 8 hours of fasting, 5 mL serum samples collected from all participants were stored at -80℃ for backup. Basic information of the enrolled study subjects was collected, including age, gender, history of smoking and drinking, blood pressure, blood glucose, lipids, and NIHSS scores of patients with AIS, as detailed in Table 1. All subjects signed an informed consent form, and the study was approved by the Ethics Committee of the second affiliated Hospital of Xi'an Medical University.

Cell culture and OGD/R model construction

SH-SY5Y cells were purchased from ATCC (USA) and cultured in DMEM medium with 10% PBS and 1% penicillin-streptomycin at 37℃, 5% CO_2. For OGD/R model construction, glucose- and serum-free DMEM medium was placed in an anaerobic environment until a large number of bubbles were visible in the medium. Then, the pretreated glucose-free and serum-free anaerobic DMEM medium was quickly added into the original medium. Cells were placed in an anaerobic box and incubated in a 37℃, humidity-saturated cell incubator for 6 hours. Afterward, cells were removed from the anaerobic box and washed once with PBS. Then, high glucose containing 10% FBS was added to the DMEM medium. The medium was placed in a 37℃, humidity-saturated cell incubator containing 5% CO_2 and continued to incubate for 24 hours for subsequent experiments.

Plasmid construction and transfection

MiR-641 mimics, miR-641 inhibitor, NC mimics, NC inhibitor, si-NC and si-MCL-1 were purchased from GenePharma (Suzhou, China). Full-length of MCL-1 was synthesized by PCR amplification and inserted into pcDNA3.1 vector to construct MCL-1 overexpressing plasmid ov-MCL-1 while pcDNA3.1 functioned as the control (ov-NC). For cell transfection, these plasmids were transfected into SH-SY5Y cells using Lipofectamine 2000 reagent (Invitrogen; Thermo Fisher Scientific, Inc., Shanghai, China) as per the manufacturer's instructions.

ELISA assay detected IL-1β and TNF-α level

Expression of IL-1β and TNF-α were detected by corresponding commercial ELISA kits as per the manufacturer's instructions.

Cell viability was determined by CCK-8 assay

SH-SY5Y cells treated with OGD/R at a density of 1×10^4 cells/well were inoculated in 96-well plates and incubated at 37°C. At 0, 12, 24 and 48 hours, 10 μL of CCK-8 solution was added to each well and incubated for 2 hours at 37°C protected from light. The relative cell viability was calculated by measuring the absorbance at 450 nm with an enzyme marker.

Flow cytometry analysis detected cell apoptosis

Cells were inoculated on 96-well plates at 3×10^3 cells/well and cultured in a humidified atmosphere with 5% CO_2 at 37℃. After incubation for 24 hours, 5 μL of PE and 7-AAD were added to each tube, and incubated for 2 hours under protection from light. Finally, the apoptotic cells were measured by FACSAria System (Becton-Dickinson, USA).

Real-time quantitative polymerase chain reaction (qRT-PCR) assay

Total RNAs were lysed and extracted from cells using TRIzol reagent. The concentrations of RNAs were measured by spectrophotometric method. TaqMan™ Reverse Transcription Kit was used to reverse transcribe RNAs into cDNA following the protocol. Then, the qRT-PCR amplification reaction was performed using SYBR Master Kit on a 7500 ABI system (BD Bioscience). The thermal cycles included initial denaturation at 95℃ for 10 minutes, followed by 40 cycles of 95℃ for 15 seconds and 60℃ for 1 minute. GAPDH and U6 functioned as the internal controls. For quantification of miR-641 and MCL-1, the $2^{-\triangle\triangle CT}$ method was used. The primer sequences were as listed: miR-641 forward, 5'-GGGGAAAGACATAGGATAGAGT-3',
and reverse,
5'-CAGTGCGTGTCGTGGAG-3';
U6 forward,
5'-TGCTTCGGCAGCACATATAC-3',
and reverse,
5'-AGGGGCCATGCTAATCTTCT-3';
MCL-1 forward,
5'-TCGTAAGGACAAAACGGGAC-3',
and reverse,
5'-CATTCCTGATGCCACCTTCT-3';
GAPDH forward,
5'-GGGCTCATCTGAAGGGTGGTGCTA-3',
and reverse,
5'-GTGGACGCTGGGATGATGTTCTGG-3'.

Western blot assay

Total proteins were extracted from cells using RIPA lysis buffer and quantified by BCA method. Then, 12% SDS-PAGE was used to separate proteins. After transferring proteins into PVDF membranes, the membranes were blocked in 5% skim milk for 2 hours at room temperature. Afterward, the membranes were incubated with primary antibodies at 4℃ overnight. Then, the secondary antibody was added on the membranes and incubated for 2 hours at room temperature. Finally, the enhanced ECL solution was added and the bands were visualized by Chemi Imager System. The integrated density value was evaluated by ImageJ software.

RESULTS

Clinical features of AIS patients and healthy controls enrolled in this study

As shown in Table 1, there were no significant differences in age, gender, alcohol drinking, smoking, diabetes history, total cholesterol (TC), triglyceride (TG), low-density lipoprotein (LDL), and high-density lipoprotein (HDL) between the two groups. However, there were significant differences in hypertension history between the two groups.

The qRT-PCR demonstrated that miR-641 expression was significantly up-regulated while MCL-1 was down-regulated in serum samples from AIS patients compared with healthy controls (Figure 1A and 1B). The receiver operating characteristic (ROC) results showed that miR-641 and MCL-1 expressions could discriminate AIS patients from healthy controls with high sensitivity, specificity, and accuracy (Figure 1C and 1D). Moreover, correlation analysis elucidated that miR-641 was positive while MCL-1 level was negatively correlated with NIHSS scores in ASI patients (Figure 1E and 1F).

OGD/R treatment hindered cell proliferation and triggered apoptosis and inflammation response in SH-SY5Y cells

OGD/R-triggered SH-SY5Y cell was built to construct an ischemic stroke *in vitro* model. As shown in Figure 2A, after OGD treatment, miR-641 was gradually increased in a time-dependent manner. On the contrary, MCL-1 mRNA and protein expressions gradually decreased with the prolonging of time (Figure 2B and 2C). Moreover, the CCK-8 and flow cytometry analysis demonstrated that OGD treatment hindered SH-SY5Y cell viability but promoted apoptosis in a time-dependent way (Figure 2D and 2E). Also, the ELISA assay illustrated that levels of pro-inflammatory cytokines IL-1β and TNF-α were significantly increased after 6, 12, and 24 hours OGD/R treatment. Collectively, OGD/R treatment could inhibit SH-SY5Y cell proliferation but induced apoptosis and inflammation response, suggesting the ischemic stroke *in vitro* model was successfully constructed.

MiR-641 aggravated OGD/R-triggered SH-SY5Y cell apoptosis and inflammation

After disturbing miR-641 expression in OGD/R-treated SH-SY5Y, the transfection efficacy was detected. As depicted in Figure 3A, miR-641 mimics transfection could increase miR-641 expression while miR-641 inhibitor could reduce miR-641 expression. Moreover, the CCK-8 and flow cytometry analysis in Figure 3B-3D elucidated that up-regulation of miR-641 could suppress OGD/R-treated SH-SY5Y cell proliferation but prominently facilitate apoptosis. Conversely, miR-641 silencing could motivate OGD/R-triggered SH-SY5Y cell proliferation but restrain apoptosis compared with controls. Moreover, the ELISA assay in Figure 3E and 3F declared that miR-641 mimic could increase IL-1β and

Table 1. Clinicopathological features of ASI patients and healthy controls.

		AIS (n = 51)	Healthy (n = 50)	p-value
Age (years)		62.5 ± 3.8	63.7 ± 4.1	0.1305
Gender	Male	29	26	0.6237
	Female	22	24	
Alcohol drinking		4	5	0.7037
Smoking history		11	12	0.7708
Hypertension history		36	3	< 0.0001
Diabetes history		23	21	0.7536
TC (mmol/L)		4.72 ± 1.06	4.69 ± 0.94	0.8806
TG (mmol/L)		1.59 ± 0.79	1.53 ± 0.92	0.7261
LDL (mmol/L)		2.97 ± 0.91	2.96 ± 0.80	0.9533
HDL (mmol/L)		1.15 ± 0.34	1.28 ± 0.37	0.0692
NIHSS scores				/
1 ~ 4		15	/	
5 ~ 15		27	/	
16 ~ 25		9	/	

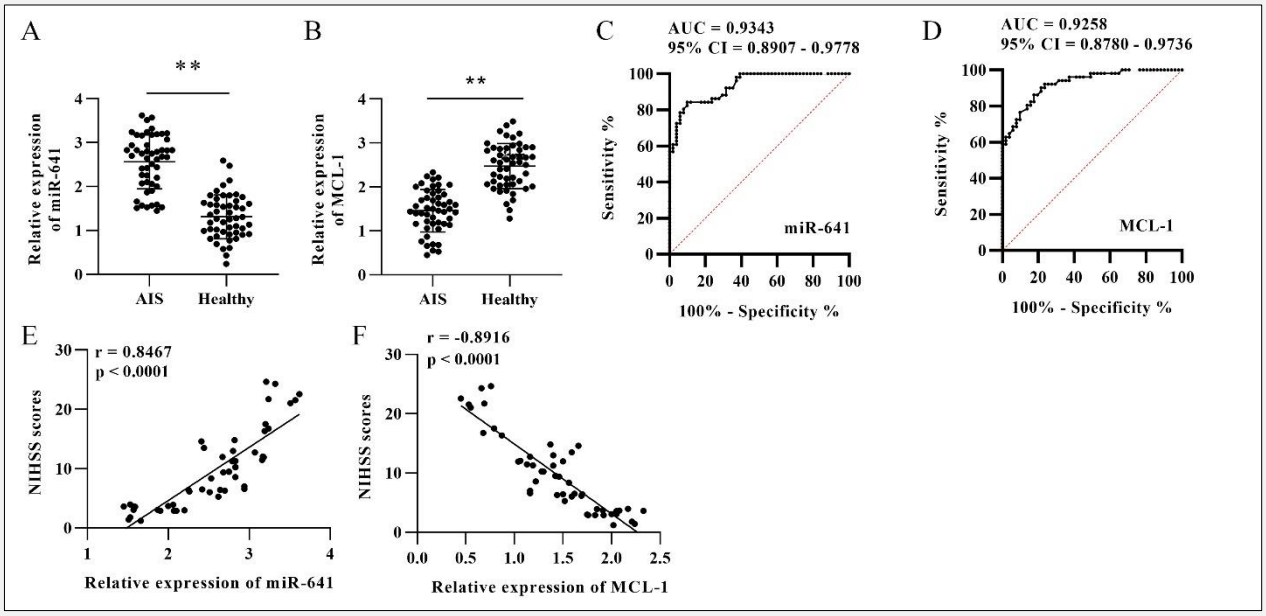

Figure 1. Clinical significance of miR-641 and MCL-1 in AIS.

(A) Expression level of miR-641 in serum samples from AIS patients and healthy controls. (B) Expression level of MCL-1 in serum samples from AIS patients and healthy controls. (C) ROC results of miR-641 in discriminating AIS patients from health controls. (D) ROC results of MCL-1 in discriminating AIS patients from health controls. (E) Correlation analysis between miR-641 level and NIHSS scores. (F) Correlation analysis between MCL-1 level and NIHSS scores.

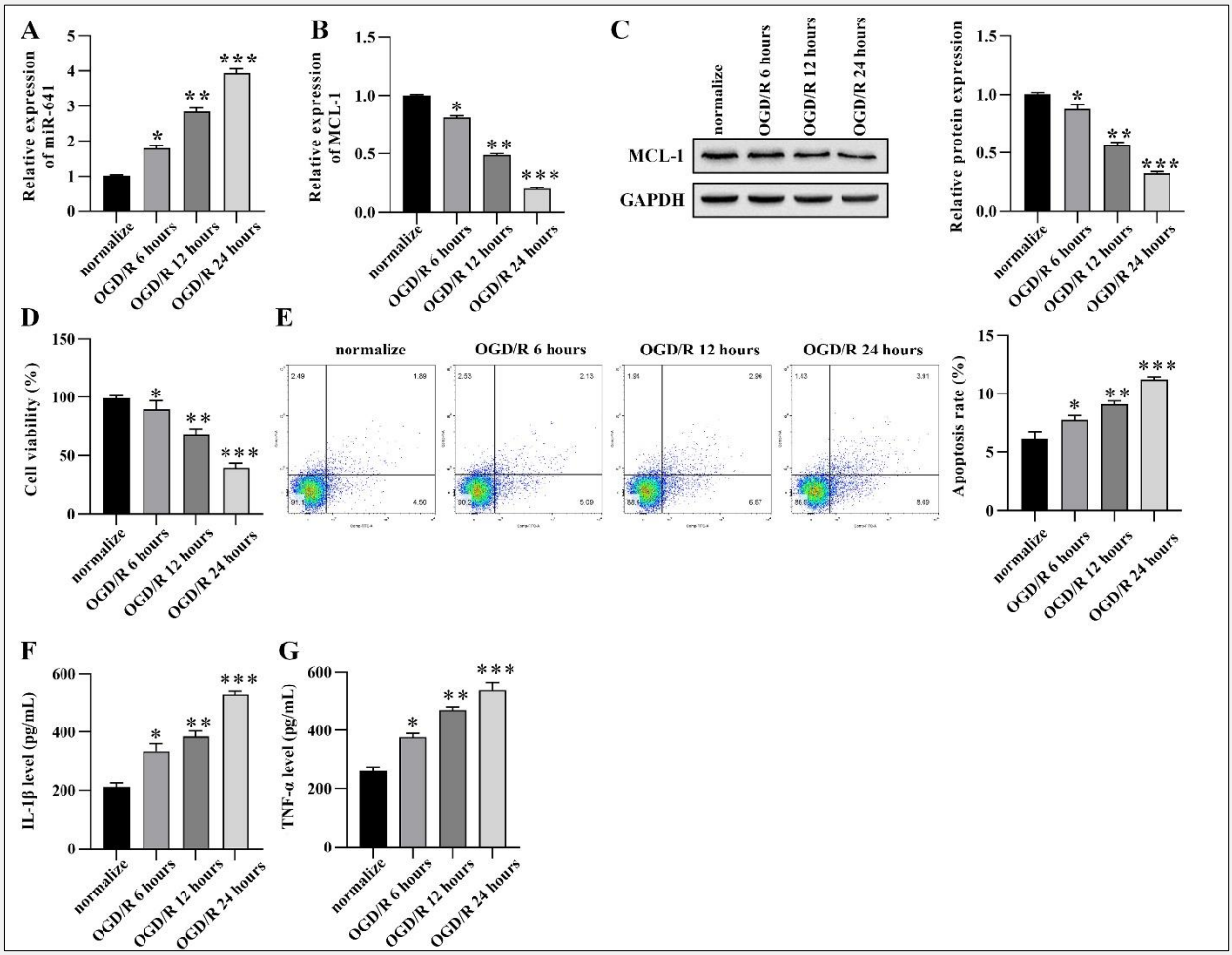

Figure 2. Effects of OGD/R treatment on SH-SY5Y cell proliferation, apoptosis, and inflammation.

(A) miR-641 level after 0, 6, 12 and 24 hours of OGD treatment. (B) MCL-1 mRNA level after 0, 6, 12 and 24 hours of OGD treatment. (C) MCL-1 protein level after 0, 6, 12 and 24 hours of OGD treatment. (D) Effects of OGD/R treatment on SH-SY5Y cell viability was measured by CCK-8 assay. (E) Effects of OGD/R treatment on SH-SY5Y cell apoptosis was detected by flow cytometry analysis. (F) IL-1β level after 0, 6, 12 and 24 hours of OGD treatment. (G) TNF-α level after 0, 6, 12 and 24 hours of OGD treatment.

TNF-α levels; whereas, inhibition of miR-641 could decrease IL-1β and TNF-α levels. Collectively, the results above verified that miR-641 could exacerbate OGD/R-triggered SH-SY5Y cell apoptosis and inflammation.

MCL-1 was a downstream target of miR-641

The online bioinformatics tool PITA predicted the putative binding sites between MCL-1 and miR-641, as shown in Figure 4A. RNA pull-down results in Figure 4B demonstrated that MCL-1 level was abundantly expressed in the Bio-miR-641 group compared with Bio-NC group. Meanwhile, dual-luciferase reporter assay illustrated that the luciferase activity was significantly decreased after co-transfection with MCL-1-WT and miR-641 mimics compared with MCL-1-WT and NC mimics transfection group (Figure 4C). However, there were no significant differences in MCL-1-Mut transfection groups. Furthermore, the effects of miR-641 mimics or inhibitor on MCL-1 was determined in Figure 4D. The results presented increased levels of MCL-1 in the miR-641 inhibitor group while decreased levels of MCL-1 in miR-641 mimics-transfection group. In short, these results verified that MCL-1 was a downstream target gene of miR-641.

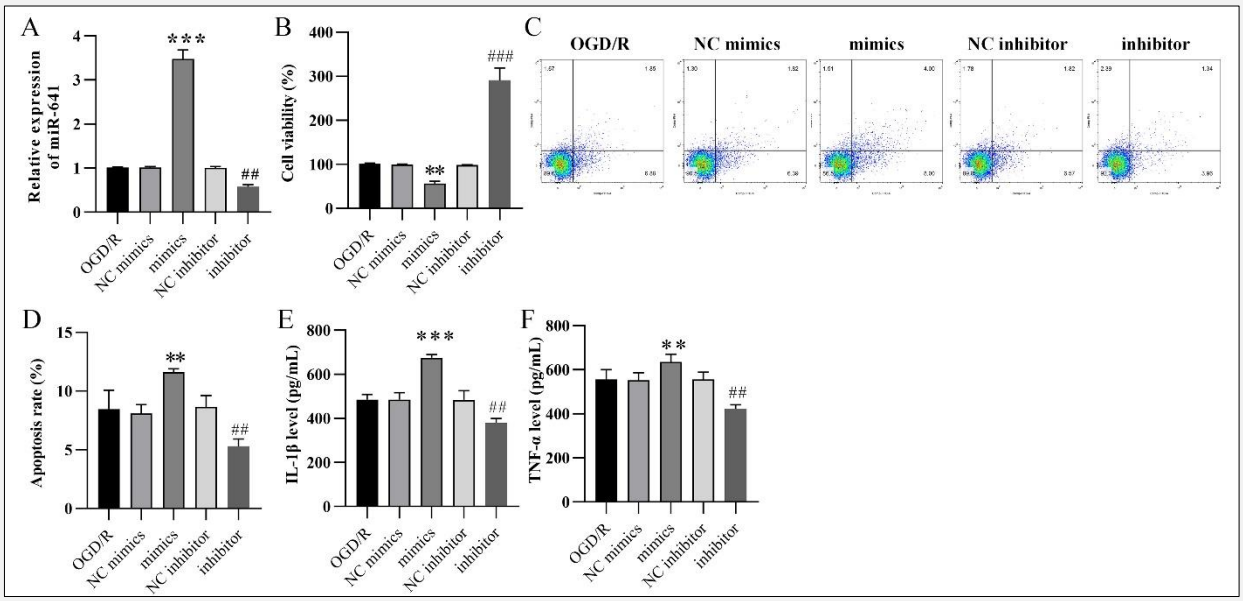

Figure 3. Effect of aberrant expressions of miR-641 on OGD/R-induced SH-SY5Y cell proliferation, apoptosis and inflammation.

(A) Transfection efficacy of miR-641 in OGD/R-triggered SH-SY5Y cells. (B) Effect of miR-641 transfection on OGD/R-triggered SH-SY5Y cell viability. (C - D) Effect of miR-641 transfection on OGD/R-triggered SH-SY5Y cell apoptosis. (E) Effect of miR-641 transfection on IL-1β level in OGD/R-induced SH-SY5Y cells. (F) Effect of miR-641 transfection on TNF-α level in OGD/R-induced SH-SY5Y cells.

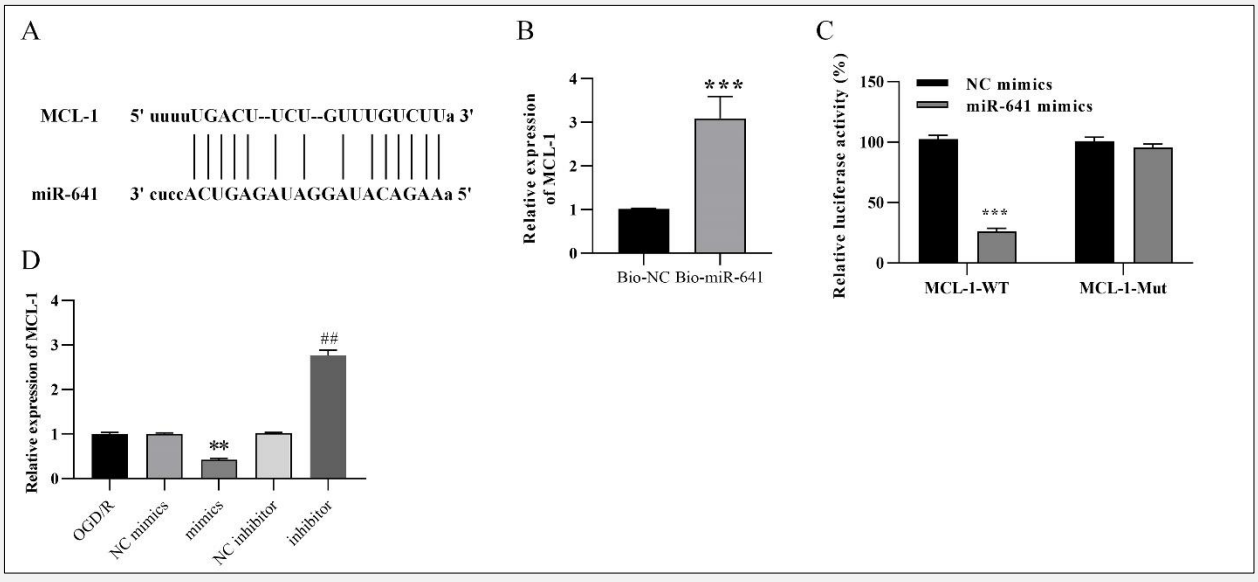

Figure 4. MCL-1 was a downstream target of miR-641.
(A) Online bioinformatic tool PITA predicted the putative binding sites between miR-641 and MCL-1. (B) RNA pull-down analysis verified the binding relationship between miR-641 and MCL-1. (C) A dual-luciferase reporter assay was conducted. (D) Effects of miR-641 transfection on MCL-1 expression.

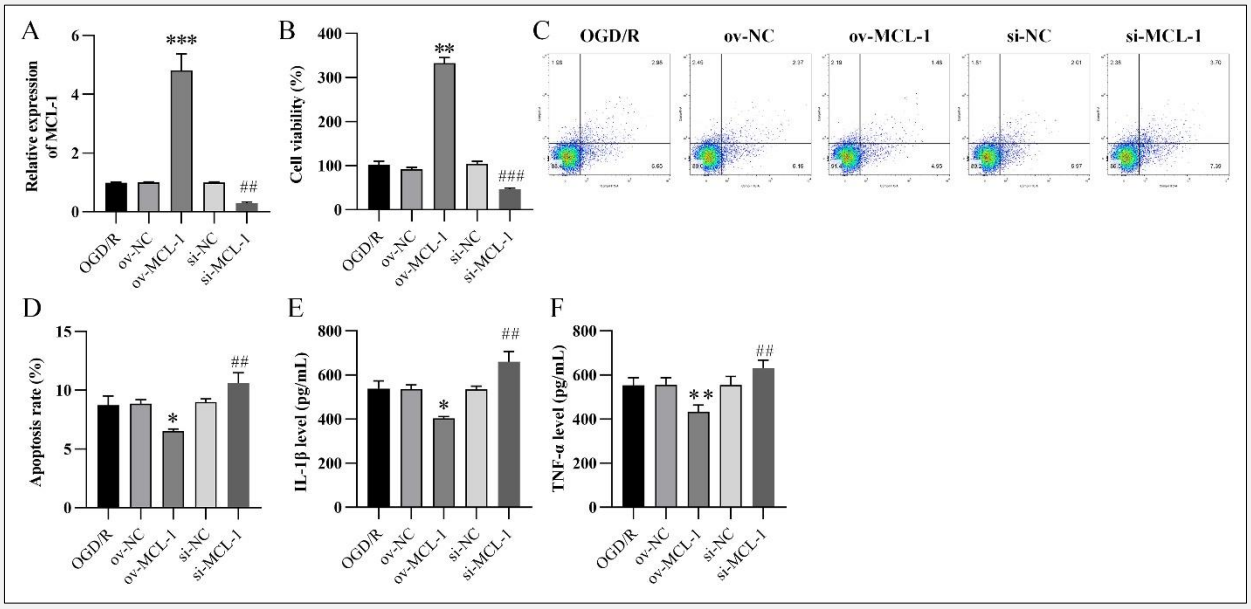

Figure 5. MCL-1 hindered OGD/R-triggered SH-SY5Y cell apoptosis and inflammation.

(A) Transfection efficiency of MCL-1 was determined by qRT-PCR analysis. (B) Effects of MCL-1 transfection on OGD/R-triggered SH-SY5Y cell viability. (C - D) Effects of MCL-1 transfection on OGD/R-triggered SH-SY5Y cell apoptosis. (E) Effects of MCL-1 transfection on IL-1β level in OGD/R-triggered SH-SY5Y cells. (F) Effects of MCL-1 transfection on TNF-α level in OGD/R-triggered SH-SY5Y cells.

MCL-1 was a key regulator in OGD/R-triggered SH-SY5Y cell proliferation, apoptosis, and inflammation

As shown in Figure 5A, after overexpressing or silencing MCL-1, the transfection efficacy was subsequently confirmed. The qRT-PCR data illustrated that MCL-1 expression was down-regulated by si-MCL-1 but up-regulated by ov-MCL-1, suggesting the transfection was successful. Furthermore, the cell viability and apoptosis assays in Figure 5B - 5D elucidated that MCL-1 overexpressing facilitated OGD/R-treated SH-SY5Y cell proliferation but restrained apoptosis. Meanwhile, silencing of MCL-1 presented the opposites effects on SH-SY5Y cells compared with ov-MCL-1. Afterward, the inflammation response of MCL-1 transfection on OGD/R-triggered SH-SY5Y cells was evaluated by ELISA assay. As shown in Figures 5E and 5F, IL-1β and TNF-α levels were remarkably increased in si-MCL-1 group while it was decreased in ov-MCL-1 group compared with si-NC or ov-NC groups.

MiR-641 regulated OGD/R-triggered SH-SY5Y cell proliferation, apoptosis, and inflammation response via MCL-1/Wnt/β-catenin pathway

To confirm the role of the miR-641/MCL-1/Wnt/β-catenin axis in OGD/R-triggered injury, we co-transfection with miR-641 and MCL-1 into SH-SY5Y cells. As depicted in Figure 6A, miR-641 mimics could decrease MCL-1 expression, while the decrease could be abolished by co-transfection with ov-MCL-1. Meanwhile, miR-641 inhibitor could increase MCL-1 level; whereas, the increase could be partially reversed by si-MCL-1 transfection. Moreover, the cell viability and ELISA assays in Figure 6B demonstrated that the inhibitory effect on OGD/R-triggered SH-SY5Y cell proliferation induced by miR-641 mimics could be rescued by ov-MCL-1. Meanwhile, the cell viability could be promoted by miR-641 inhibitor; however, the promotion could be abolished by co-transfection with si-MCL-1. On the contrary, up-regulation of miR-641 induced apoptosis and inflammation in OGD/R-triggered SH-SY5Y cells could be partially counteracted by ov-MCL-1 (Figure 6C-6H). Meanwhile, the inhibition in OGD/R-triggered SH-SY5Y cell apoptosis and inflammation response induced by miR-641 inhibitor could be reversed by si-MCL-1 as well (Figure 6C-6H).

DISCUSSION

The pathophysiological changes in ischemic stroke include many processes, including calcium imbalance, toxic effects of excitatory neurotransmitters, free radi-

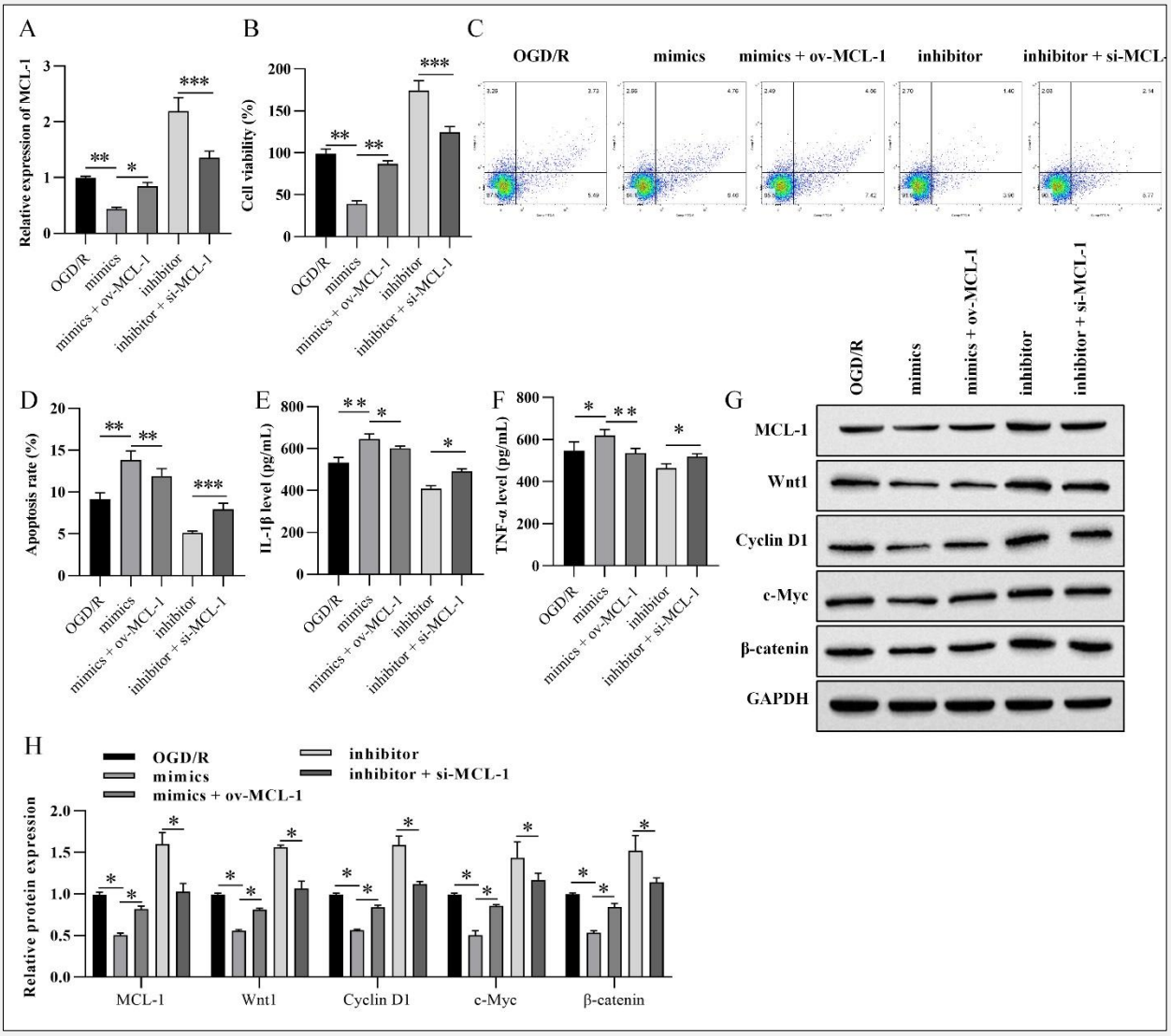

Figure 6. miR-641 aggravated OGD/R-treated SH-SY5Y cell apoptosis and inflammation response via regualting MCL-1/Wnt/β-catenin pathway.

(A) MCL-1 expressions after co-transfection with miR-641 and MCL-1. (B) Effect of miR-641 and MCL-1 co-transfection on OGD/R-induced SH-SY5Y cell viability. (C - D) Effect of miR-641 and MCL-1 co-transfection on OGD/R-induced SH-SY5Y cell apoptosis. (E) Effect of miR-641 and MCL-1 co-transfection on IL-1β level in OGD/R-induced SH-SY5Y cells. (F) Effect of miR-641 and MCL-1 co-transfection on TNF-α level in OGD/R-induced SH-SY5Y cells. (G) Effects of miR-641 and MCL-1 co-transfection on MCL-1, Wnt1, Cyclin D1 and c-Myc protein expressions.

cal-mediated cytotoxicity, inflammatory responses, and disruption of the blood-brain barrier [17]. These complex physiological processes interact with each other in time and space. In the short time after an ischemic stroke, blood flow to the brain tissue in the ischemic region is rapidly reduced leading to irreversible damage, resulting in brain cell death [18]. If the ischemic state is not eliminated within a short period, a severe ischemic infarct will develop, and irreversible damage to neurons will occur due to the complete loss of glucose and oxygen supply [19]. Therefore, it is essential to improve glucose metabolism and control neuronal apoptosis to improve ischemic injury.

After OGD treatment, neuronal cells reduce glucose uptake and lactate production, exacerbating apoptosis [20]. In the hypoxic state, disturbance of energy metabolism

and depletion of ATP in neurons will lead to dysfunction of energy-dependent ion pumps, followed by imbalance of intra- and extracellular ion gradients due to insufficient oxygen and glucose supply, resulting in acute neuronal injury [21]. Although restoring oxygen restores organ function during reperfusion, many oxygen radicals are also generated [22]. These factors acting on top of each other will lead to further damage to neural tissue. In addition, glial cells and peripheral inflammatory cells are also involved in the pathogenesis of ischemic stroke [23]. After ischemic stroke, the levels of many inflammatory factors and chemokines are upregulated, leading to increased permeability of the blood-brain barrier and infiltration of monocytes and macrophages into the area of injury [24]. The cytokines released by these inflammatory cells and glial cells further aggravate the brain tissue damage, of which neuronal apoptosis is one of the manifestations. In our study, OGD/R-triggered SH-SY5Y cells were used to construct AIS in vitro model. Under OGD/R conditions, SH-SY5Y cell viability was inhibited while apoptosis and inflammation response was triggered. Meanwhile, OGD/R treatment induced an increased level of miR-641 and decreased MCL-1 in SH-SY5Y cells. Furthermore, our experiments validated that miR-641 knockdown or MCL-1 overexpressing could reduce apoptosis and inflammatory responses in neurons after ischemic stroke. To further investigate in-depth the potential mechanisms, we hypothesized that MCL-1 might be the target of miR-641 by bioinformatics approach prediction. Dual-luciferase and RNA pull-down assays confirmed the binding relationship between miR-641 and MCL-1. To further verify the interaction between miR-641 and MCL-1, we further transfected si-MCL-1 and ov-MCL-1 alone or together with miR-641 inhibitor and miR-641 mimics in OGD-treated neuronal cells to assess neuronal apoptosis and inflammation. miR-641 on OGD/R-treated apoptosis and inflammation in SH-SY5Y cells after OGD treatment was ameliorated by MCL-1 overexpression. These results suggest a role for MCL-1 as its direct target in miR-641 in regulating neuronal injury in OGD-treated neurons. Moreover, activation of the Wnt/β-catenin pathway was reported to participate in ischemic stroke progression [25-27]. Previous studies also verified that MCL-1 could directly regulate the Wnt/β-catenin pathway [28,29]. In the present study, we used rescue experiments to confirm that miR-641 could exacerbate OGD/R-triggered SH-SY5Y cell injury via the MCL-1/Wnt/β-catenin pathway.

In summary, this study reveals the regulatory role of the miR-641/MCL-1/Wnt/β-catenin axis in OGD/R-induced SH-SY5Y cell injury, providing a new target for the treatment of AIS.

Source of Funds:

The present study was funded by Science and Technology innovation Platform of Shaanxi Key Laboratory of Brain Disorders, Xi'an Medical University, Grant No.: 20NBZD01, Shaanxi Social Development Science and Technology Plan, Grant No.: 2021SF-271), Shaanxi Provincial Education Department Service for Local Scientific Research Program 2022, and Hospital fund of the Second Affiliated Hospital of Xi'an Medical University, Grant No.: 19KY0110.

Declaration of Interest:

All authors declare that there are no conflicts of interests in this study.

References:

1. Tan YK, Goh C, Leow AST, et al. COVID-19 and ischemic stroke: a systematic review and meta-summary of the literature. J Thromb Thrombolysis 2020;50(3):587-95. (PMID: 32661757)

2. Sun MS, Jin H, Sun X, et al. Free radical damage in ischemia-reperfusion injury: an obstacle in acute ischemic stroke after revascularization therapy. Oxid Med Cell Longev 2018;2018:3804979. (PMID: 29770166)

3. Zhao B, Shi QJ, Zhang ZZ, Wang SY, Wang X, Wang H. Protective effects of paeonol on subacute/chronic brain injury during cerebral ischemia in rats. Exp Ther Med 2018;15(4):3836-46. (PMID: 29563983)

4. Nunomura A, Perry G. RNA and oxidative stress in Alzheimer's disease: focus on microRNAs. Oxid Med Cell Longev 2020; 2020:2638130. (PMID: 33312335)

5. Zhao YS, Zheng RY, Chen J, Ning D. CircRNA CDR1as/miR-641/HOXA9 pathway regulated stemness contributes to cisplatin resistance in non-small cell lung cancer (NSCLC). Cancer Cell Int 2020;20:289. (PMID: 32655321)

6. Wang LW, Li XB, Liu Z, Zhao LH, Wang Y, L Yue L. Long non-coding RNA OIP5-AS1 promotes proliferation of gastric cancer cells by targeting miR-641. Eur Rev Med Pharmacol Sci 2019;23(24):10776-84. (PMID: 31858545)

7. Zhang FH, Xu Y, Ye WF, Jiang JT, Wu CP. Circular RNA S-7 promotes ovarian cancer EMT via sponging miR-641 to up-regulate ZEB1 and MDM2. Biosci Rep 2020;40(7):BSR20200825. (PMID: 32667627)

8. Zhu YL, Liu BB,Zhang P, Zhang J, Wang L. LncRNA TUSC8 inhibits the invasion and migration of cervical cancer cells via miR-641/PTEN axis. Cell Biol Int 2019;43(7):781-8. (PMID: 31033083)

9. Niu YL, He JH, Zhang YL, Li K, Xing CG. Effect of the circCDR1as/miR-641/XIAP regulatory axis on the proliferation and invasion of the prostate cancer PC-3 cell line. Oncol Lett 2021;21(6):469. (PMID: 33907579)

10. Li KL, Han HC, Gu WJ, Cao CY, Zheng PY. Long non-coding RNA LINC01963 inhibits progression of pancreatic carcinoma by targeting miR-641/TMEFF2. Biomed Pharmacother 2020;129: 110346. (PMID: 32559621)

11. Wu HJ, Li WH, Zhu ST, Zhang DF, Zhang MH. Circular RNA circUBAP2 regulates proliferation and invasion of osteosarcoma cells through miR-641/YAP1 axis. Cancer Cell Int 2020;20:223. (PMID: 32528231)

12. Tian Y, Gao P, Dai D, Chen L, Chu X, Mei XF. Circular RNA circSETD3 hampers cell growth, migration, and stem cell properties in bladder cancer through sponging miR-641 to upregulate PTEN. Cell Cycle 2021;20(16):1589-1602. (PMID: 34288821)

13. Li DW, Tang Z, Gao ZQ, Shen PC, Liu ZC, Dang XW. Circular RNA CDR1as exerts oncogenic properties partially through regulating microRNA 641 in cholangiocarcinoma. Mol Cell Biol 2020;40(15):e00042-20. (PMID: 32423991)

14. Zhao GL, Zhang ZH, Sun SF, Ding YL. Long non-coding RNA LINC00173 enhances cisplatin resistance in hepatocellular carcinoma via the microRNA-641/RAB14 axis. Oncol Lett 2021; 21(5):371. (PMID: 33777195)

15. Hinske LC, Heyn J, Hübner M, Rink J, Hirschberger S, Kreth S. Intronic miRNA-641 controls its host Gene's pathway PI3K/AKT and this relationship is dysfunctional in glioblastoma multiforme. Biochem Biophys Res Commun 2017;489(4):477-83. (PMID: 28576488)

16. He WZ, Chen SQ, Chen XG, Li SX, Chen WJ. Bioinformatic analysis of potential microRNAs in ischemic stroke. J Stroke Cerebrovasc Dis 2016;25(7):1753-9. (PMID: 27151415)

17. Xu H, Wang E, Chen F, Xiao JB, Wang MF. Neuroprotective phytochemicals in experimental ischemic stroke: mechanisms and potential clinical applications. Oxid Med Cell Longev 2021; 2021:6687386. (PMID: 34007405)

18. Radak D, Katsiki N, Resanovic I, et al. Apoptosis and acute brain ischemia in ischemic stroke. Curr Vasc Pharmacol 2017;15(2): 115-22. (PMID: 27823556)

19. Wang SW, Liu Z, Shi ZS. Non-coding RNA in acute ischemic stroke: mechanisms, biomarkers and therapeutic targets. Cell Transplant 2018;27(12):1763-77. (PMID: 30362372)

20. Thomaz DT, Andreguetti RR, Binder LB, et al. Guanosine neuroprotective action in hippocampal slices subjected to oxygen and glucose deprivation restores ATP levels, lactate release and glutamate uptake impairment: involvement of nitric oxide. Neurochem Res 2020;45(9):2217-29. (PMID: 32666283)

21. Lai YX, Lin PQ, Chen ML, et al. Restoration of L-OPA1 alleviates acute ischemic stroke injury in rats via inhibiting neuronal apoptosis and preserving mitochondrial function. Redox Biol 2020;34:101503. (PMID: 32199783)

22. Bhattacharyya A, Chattopadhyay R, Mitra S, Crowe SE. Oxidative stress: an essential factor in the pathogenesis of gastrointestinal mucosal diseases. Physiol Rev 2014;94(2):329-54. (PMID: 24692350)

23. Xu SB, Lu JN, Shao AW, Zhang JH, Zhang JM. Glial cells: role of the immune response in ischemic stroke. Front Immunol 2020; 11:294. (PMID: 32174916)

24. Srivastava P, Cronin CG, Scranton VL, Jacobson KA, Liang BT, Verma R. Neuroprotective and neuro-rehabilitative effects of acute purinergic receptor P2X4 (P2X4R) blockade after ischemic stroke. Exp Neurol 2020;329:113308. (PMID: 32289314)

25. Wang T, Duan YM, Fu Q, et al. IM-12 activates the Wnt-β-catenin signaling pathway and attenuates rtPA-induced hemorrhagic transformation in rats after acute ischemic stroke. Biochem Cell Biol 2019;97(6):702-8. (PMID: 31770017)

26. Wang JR, Chen TZ, Shan GZ. miR-148b regulates proliferation and differentiation of neural stem cells via Wnt/β-catenin signaling in rat ischemic stroke model. Front Cell Neurosci 2017;11: 329. (PMID: 29104534)

27. Song XM, Xue YM, Cai HR. Down-regulation of miR-181a-5p prevents cerebral ischemic injury by upregulating En2 and activating Wnt/β-catenin pathway. J Stroke Cerebrovasc Dis 2021; 30(3):105485. (PMID: 33360253)

28. Tang Y, Yang P, Zhu YF, Su Y. LncRNA TUG1 contributes to ESCC progression via regulating miR-148a-3p/MCL-1/Wnt/β-catenin axis in vitro. Thorac Cancer 2020;11(1):82-94. (PMID: 31742924)

29. Flores ML, Castilla C, Gasca J, et al. Loss of PKCδ induces prostate cancer resistance to paclitaxel through activation of Wnt/β-catenin pathway and Mcl-1 accumulation. Mol Cancer Ther 2016; 15(7):1713-25. (PMID: 27196755)